

RESEARCH LETTER

10.1002/2016GL068998

Key Points:

- Warm but modified CDW floods the continental shelf of the Bellingshausen Sea
- A cyclonic trough circulation that carries heat toward the coast is detected
- The mCDW flows westward at the shelf break, suggesting the Antarctic Slope Current

Supporting Information:

- Supporting Information S1
- Table S1
- Figure S1
- Figure S2
- Figure S3

Correspondence to:

X. Zhang,
xiyue@caltech.edu

Citation:

Zhang, X., A. F. Thompson, M. M. Flexas, F. Roquet, and H. Bornemann (2016), Circulation and meltwater distribution in the Bellingshausen Sea: From shelf break to coast, *Geophys. Res. Lett.*, 43, doi:10.1002/2016GL068998.

Received 4 APR 2016

Accepted 27 MAY 2016

Accepted article online 1 JUN 2016

Circulation and meltwater distribution in the Bellingshausen Sea: From shelf break to coast

Xiyue Zhang¹, Andrew F. Thompson¹, Mar M. Flexas², Fabien Roquet³, and Horst Bornemann⁴

¹Environmental Science and Engineering, California Institute of Technology, Pasadena, California, USA, ²Jet Propulsion Laboratory, California Institute of Technology, Pasadena, California, USA, ³Department of Meteorology, Stockholm University, Stockholm, Sweden, ⁴Alfred Wegener Institute, Helmholtz-Zentrum für Polar- und Meeresforschung, Bremerhaven, Germany

Abstract West Antarctic ice shelves have thinned dramatically over recent decades. Oceanographic measurements that explore connections between offshore warming and transport across a continental shelf with variable bathymetry toward ice shelves are needed to constrain future changes in melt rates. Six years of seal-acquired observations provide extensive hydrographic coverage in the Bellingshausen Sea, where ship-based measurements are scarce. Warm but modified Circumpolar Deep Water floods the shelf and establishes a cyclonic circulation within the Belgica Trough with flow extending toward the coast along the eastern boundaries and returning to the shelf break along western boundaries. These boundary currents are the primary water mass pathways that carry heat toward the coast and advect ice shelf meltwater offshore. The modified Circumpolar Deep Water and meltwater mixtures shoal and thin as they approach the continental slope before flowing westward at the shelf break, suggesting the presence of the Antarctic Slope Current. Constraining meltwater pathways is a key step in monitoring the stability of the West Antarctic Ice Sheet.

1. Introduction

The Southern Ocean has experienced substantial changes since the last century, including warming throughout the water column [Gille, 2008] and freshening of bottom water [Rintoul, 2007; Aoki *et al.*, 2005; Purkey and Johnson, 2013]. Close to the Antarctic coast, remote observations have shown that basal melt has become the leading process for ice shelf thinning [Pritchard *et al.*, 2012] and mass loss [Rignot *et al.*, 2013] in Antarctica. Significant glacier thinning was observed as a consequence of the ice shelf loss [Wouters *et al.*, 2015]. However, the link between ocean warming and accelerated ice shelf basal melt is less clear, mainly due to the lack of observations at high latitudes and the complicated, bathymetrically influenced continental shelf circulation.

Various studies have addressed the oceanic forcing on ice shelf basal melt. In the central Amundsen Sea, persistent flow of warm Circumpolar Deep Water (CDW) has been observed on the continental shelf [Arneborg *et al.*, 2012; Wählin *et al.*, 2013; Walker *et al.*, 2013]. There is strong evidence that shelf water here includes a modified CDW-meltwater mixture [Wählin *et al.*, 2010; Nakayama *et al.*, 2013]. Measurements in the vicinity of ice shelves allow estimations of basal melt rates, such as the Pine Island Ice Shelf [Jenkins, 1999; Dutrioux *et al.*, 2014; Nakayama *et al.*, 2013]. There are also detailed studies of the Wilkins Ice Shelf and George VI Ice Shelf in the Bellingshausen Sea [Padman *et al.*, 2012; Jenkins and Jacobs, 2008]. In the western Bellingshausen Sea, hydrographic data are limited, although these measurements indicate that warm CDW found over the continental slope in this region is both warming and shoaling over the past two decades [Schmidtke *et al.*, 2014].

Warm CDW may enter the Bellingshausen Sea through the Belgica Trough and the Latady Trough to access the ice shelf cavities (Figure 1). Many ice shelves occupy the coast of the Bellingshausen Sea, all of which show positive basal melt rate [Rignot *et al.*, 2013] and volume loss in the last two decades [Paolo *et al.*, 2015]. The ice shelves east of 80°W have been relatively well studied and monitored [Jacobs *et al.*, 1996; Jenkins and Jacobs, 2008; Padman *et al.*, 2012]. Less is known about the circulation and melting of the two ice shelves west of 80°W. For example, although the Venable Ice Shelf covers a smaller area, its basal melt rate is higher than that of the more extensive Wilkins Ice Shelf [Rignot *et al.*, 2013]. Numerical simulations have shown high concentration of melt water in the Belgica Trough from Bellingshausen Sea ice shelves [Nakayama *et al.*, 2014],

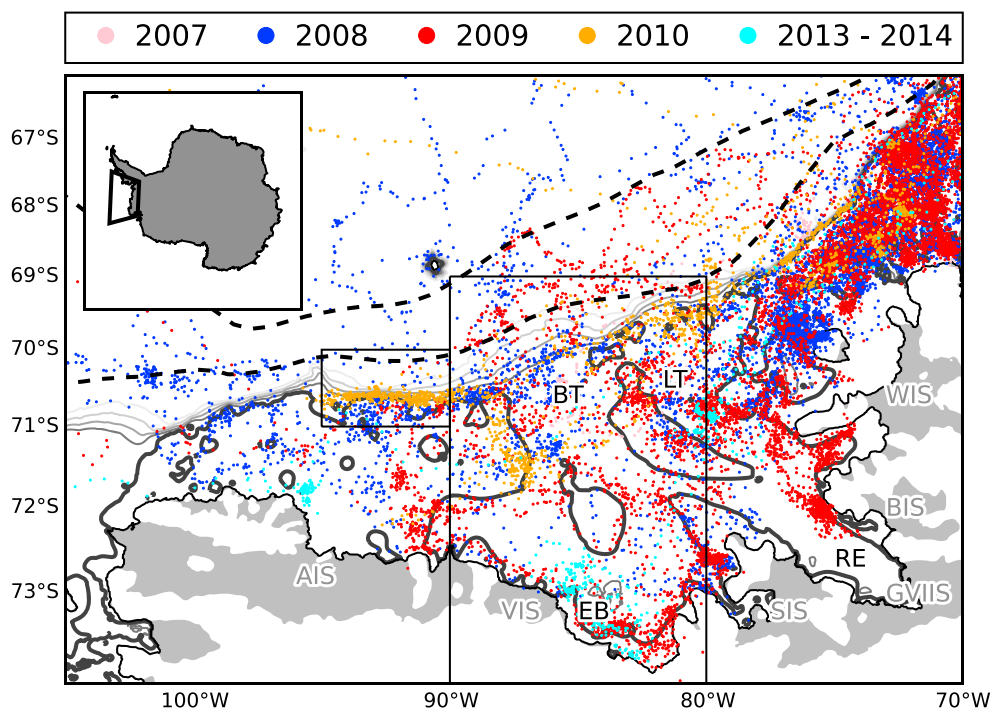


Figure 1. Map of western and central Bellingshausen Sea. Dots show the locations of all Marine Mammals Exploring the Oceans Pole to Pole conductivity-temperature-depth (MEOP-CTD) profiles used in this study. Colors indicate the different years. Contours show 0, 500 (thickened), 1000, 1500, 2000, and 2500 m isobaths from International Bathymetric Chart of the Southern Ocean bathymetry [Arndt *et al.*, 2013]. Grey shadings indicate the ice shelves in the region: Abbot Ice Shelf (AIS), Venable Ice Shelf (VIS), Stange Ice Shelf (SIS), George VI Ice Shelf (GVIIS), Bach Ice Shelf (BIS), and Wilkins Ice Shelf (WIS). Other features include Belgica Trough (BT), Latady Trough (LT), Eltanin Bay (EB), and Ronne Entrance (RE). Dashed lines are the Southern Antarctic Circumpolar Current (ACC) front and the Southern Boundary defined by Orsi *et al.* [1995]. The black boxes show the regions in Figures 2 and 3. The insert shows the location of the studied region in Antarctica.

and a weak cyclonic circulation on the continental shelf [Holland *et al.*, 2010]. Here hydrographic data are used to understand both the water modification processes on the shelf and the circulation in the Belgica Trough.

At the shelf break, the frontal separation of offshore warm, salty CDW and colder, fresher shelf waters is related to the westward circulation of the Antarctic Slope Current (ASC) [Jacobs, 1991]. The ASC is not apparent along the western side of the Antarctic Peninsula, where the Southern Boundary of the ACC may flow unimpeded onto the continental shelf. Yet the ASC is frequently seen in the Amundsen Sea suggesting that the ASC's initiation is found somewhere in the Bellingshausen Sea. Observations of the exact location of the ASC's formation and its subsequent along-stream development are limited.

Although there has been a significant augmentation of oceanic observations in the Bellingshausen Sea by Argo floats, these hydrographic profiles are mostly north of the continental shelf break and are limited by the extent of seasonal sea ice. On the continental shelf and especially in the Belgica Trough, hydrographic data remain limited. Animal-borne observations have become more prevalent in the last decade, mainly in high-latitude regions by instrumented seals. These seals travel great distances in open water and under sea ice as they dive to between 500 and 2000 m depth. Water properties are sampled during the nearly vertical ascent phase of seal dives [Boehme *et al.*, 2009]. Calibrated data collected by the conductivity-temperature-depth satellite relay data loggers (CTD-SRDLs) efficiently contribute to an improved state estimate of the Southern Ocean circulation [Roquet *et al.*, 2013]. While the seal data presented here have irregular spatial and temporal sampling, they are the best available observations that cover, from the shelf break to the coast, a significant part of the Bellingshausen Sea continental shelf region. They also potentially provide a relatively long time series to examine evolving shelf break properties that shed light on the variability of the ASC in this region. In section 2 we describe the hydrographic data; results are presented in section 3. In section 4 we discuss how offshore properties as well as the continental shelf circulation and bathymetry influence the distribution of the ice shelf meltwater.

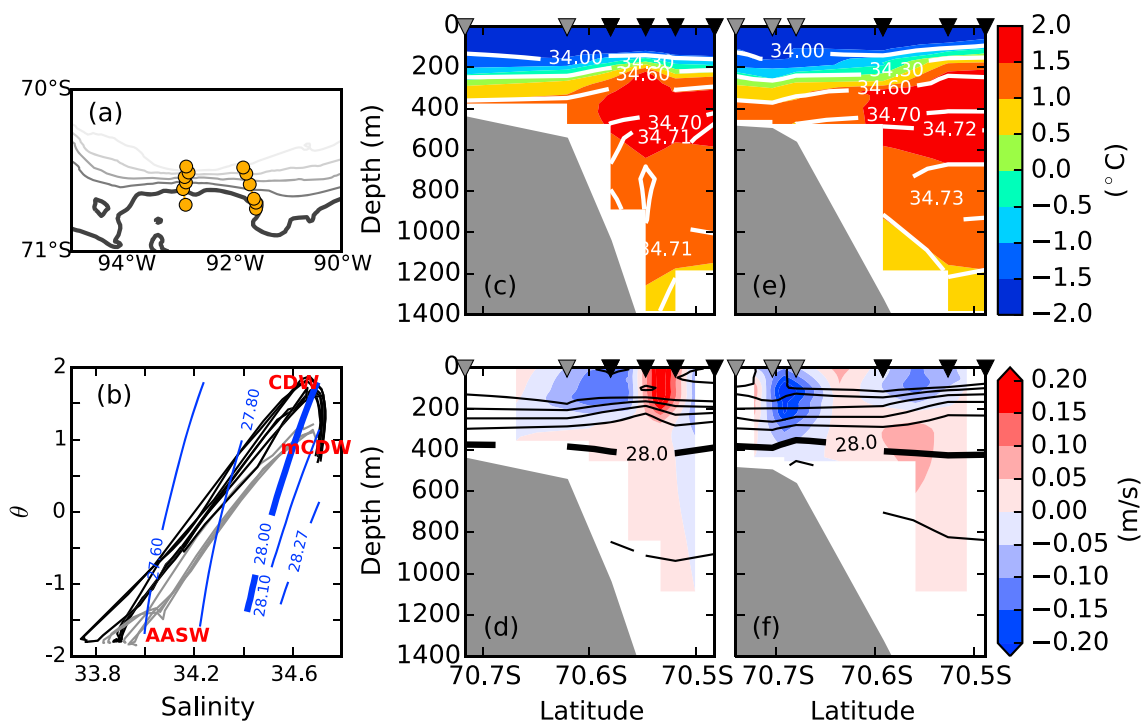


Figure 2. Depth-latitude cross-shelf cross-slope section at the shelf break. (a) Map of the boxed region in Figure 1. (b) θ - S diagram of the sections' profiles, with on-shelf ones in grey and offshore in black. The blue lines show select neutral density surfaces. Water masses are labeled in red. See the text for details. (c) Temperature ($^{\circ}\text{C}$, colors) and salinity (contours) for the section near 93°W in August 2010. (d) Geostrophic velocity (m s^{-1} , colors) referenced to the lowest data level and neutral density (kg m^{-3} , contours) for the section near 93°W in August 2010. The contour interval is 0.1 kg m^{-3} . Positive velocity indicates eastward flow. (e and f) The same as Figures 2c and 2d but for the section near 92°W in June 2010. Triangles indicate the latitude of the profiles.

2. Data

We analyze data from the Marine Mammals Exploring the Oceans Pole to Pole (MEOP-CTD) database [Roquet *et al.*, 2013] (see <http://www.meop.net/>). These data are collected by southern elephant seals (*Mirounga leonina*) and crabeater seals (*Lobodon carcinophaga*) instrumented with CTD-SRDLs at several sites west of the Antarctic Peninsula. The data set provides extensive coverage in the Bellingshausen Sea region both temporally and spatially (Figure 1). The seals are able to dive beneath sea ice and transmit data in open leads when the coastal ocean is almost inaccessible to ships.

All data are subject to temperature and salinity calibration. Following the MEOP standard, calibration was conducted based on historical data in nearby regions [Roquet *et al.*, 2011]. The calibrated data have estimated uncertainties of $\pm 0.02^{\circ}\text{C}$ for temperature and ± 0.02 practical salinity unit (psu) for salinity.

There are a total of 19,893 seal dives used in the Bellingshausen Sea region in this study. The data span the years 2007 to 2010 [Costa *et al.*, 2008; McIntyre *et al.*, 2014], and austral summer of 2013–2014 (supporting information Table S1). More than 85% of the data were collected in austral autumn and winter (Figure S1). Data density is the highest on the continental shelf north of the Wilkins Ice Shelf. The coastal and shelf break regions also tend to have higher than average data density (Figure 1). Although north of the Venable Ice Shelf and the Abbot Ice Shelf have the sparsest data coverage on the continental shelf, this data set represents the most comprehensive survey of near-shore water mass properties in this region of the Bellingshausen Sea.

3. Results

The full data set will be used to explore water mass pathways over the continental shelf. First, though, we begin by considering subsets of the data, as hydrographic sections, that show water mass characteristics at the continental shelf break and at the major troughs.

Typical cross-shelf and cross-slope hydrographic sections in the western Bellingshausen Sea, collected in austral winter 2010, show a surface mixed layer of near-freezing temperature extending to a depth that varies between 100 and 150 m (Figure 2). This mixed layer is composed of the coldest Antarctic Surface Water

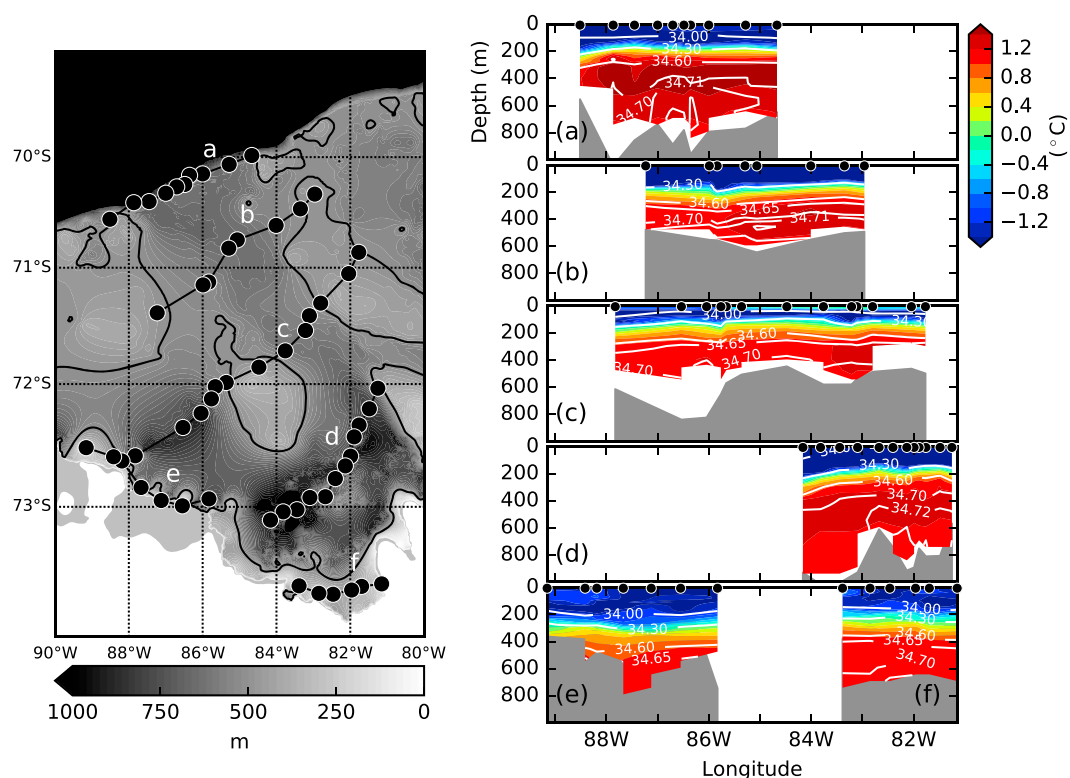


Figure 3. (left) Depth of the Belgica Trough (m) and position of synoptic seal sections. The background shading of the map only shows bathymetry shallower than 1000 m, with the 500 m bathymetry highlighted in black line. Black circles indicate profile locations. (right) Potential temperature ($^{\circ}\text{C}$, colors) and salinity (contours) sections in the Belgica Trough. Sections taken in (a) April 2010, (b) December 2013, (c) February 2008, (d) December 2013, (e) March 2008, and (f) March 2009.

(AASW, $\gamma^n < 28.00 \text{ kg m}^{-3}$), which extends to a depth of approximately 400 m, consistent with *Whitworth et al.* [1998]. The warmest and saltiest water mass, Circumpolar Deep Water (CDW, $28.00 < \gamma^n < 28.27 \text{ kg m}^{-3}$), lies offshore between 400 m and 800 m. Offshore, the θ_{max} associated with Upper CDW is $\sim 2^{\circ}\text{C}$, and the S_{max} associated with Lower CDW is ~ 34.73 psu. This distribution agrees with the climatological position of the Southern Boundary of ACC [*Orsi et al.*, 1995], found just offshore of the continental shelf break. Our data set does not contain Antarctic Bottom Water (AABW) ($\gamma^n > 28.27 \text{ kg m}^{-3}$, $\theta > -1.85^{\circ}\text{C}$).

The neutral density surfaces in Figure 2 reflect a vertically sheared geostrophic flow along the shelf break under the assumption of thermal wind balance. It is not possible to determine a reference velocity directly from the seal data, but we choose to reference to the bottom since there is no evidence of a dense water outflow over the shelf that would give rise to strong bottom currents. There may still be a barotropic component of the flow that is not resolved. Assuming no motion at the bottom, the shear gives rise to a westward flow near the surface at the shelf break with weaker velocities at depth and a weak eastward current farther offshore.

Over the continental shelf, the θ_{max} and S_{max} of the CDW are reduced. This modified CDW (mCDW) is both colder and fresher than the CDW found offshore (Figure 2b). Yet temperatures as warm as 1°C extend onshore, past the shelf break, and spread over the continental shelf. To investigate the on-shelf distribution of mCDW, we consider five synoptic hydrographic sections (e.g., nearly consecutive seal dives) that cross the Belgica Trough, starting near the shelf break and moving toward the coast (Figure 3). Although these sections are from different time periods, some general trends are common below the thermocline.

Water warmer than 1°C is always present at depth. Cross-trough (east-west) gradients of θ and S are observed in every section, although the gradient weakens closer to the coast. Additional modifications are found in the along-trough direction. The temperature of the θ_{max} , warmest at the continental shelf break ($\theta \sim 1.4^{\circ}\text{C}$), is found at ~ 400 m, with its salinity maximum at ~ 700 m. Moving closer to the coast, the θ_{max} is confined to the

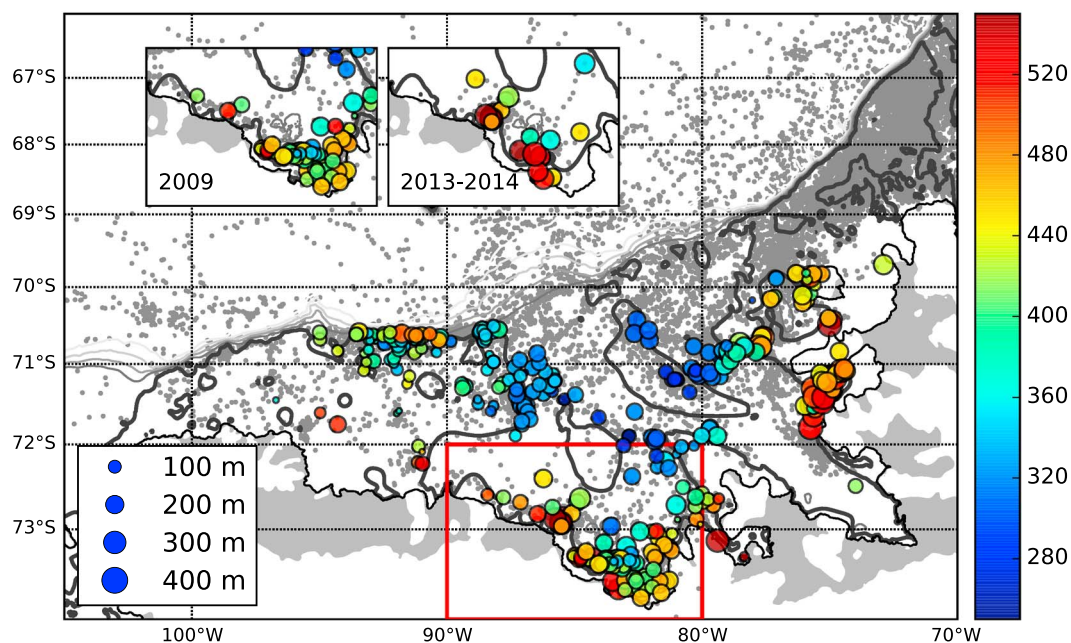


Figure 4. Map of all casts that do (color) and do not (grey) fall within the Gade envelope; see text for details. Shallow casts are removed from Gade envelope analysis. The color indicates the mean meltwater mixture layer depth (m), and the sizes of the circles show the meltwater mixture layer thickness. The inserts show the Eltanin Bay region (red box) in 2009 and winter 2013–2014.

eastern side of the Belgica Trough (Figures 3a–3d). At the western side of the Belgica Trough, the middepth temperature maximum is eroded. The east-west difference in water mass characteristics suggests a cyclonic boundary current system within the trough with mCDW entering at the shelf break. This mCDW is modified slightly by mixing along the trough, but most of the modification occurs close to the coast. This can be seen in Figures 3e and 3f, which show a complete erosion of the middepth θ_{\max} (Figure 3f). We also see a modification in salinity along the eastern boundary of the trough; however, given the instrumental uncertainty of 0.02 psu, the signal is marginal.

The contribution of ice shelf meltwater on mCDW is analyzed using the Gade line, defined as [Gade, 1979; Jenkins, 1999; Wåhlin et al., 2010]

$$\theta(S) = \theta_{\text{ocean}} + L_f(1 - S_{\text{ocean}}/S)/C_p, \quad (1)$$

where $L_f = 334 \text{ kJ kg}^{-1}$ is the latent heat of fusion, $C_p = 3.97 \text{ kJ kg}^{-1} \text{ K}^{-1}$ is specific heat of sea water, and $\theta_{\text{ocean}} = 1.2 \pm 0.1^\circ\text{C}$ and $S_{\text{ocean}} = 34.7 \text{ psu}$ are used as the characteristic θ and S for mCDW on shelf. By definition, θ - S values that lie along the Gade line obtain their characteristics from a mixture of ice shelf water and mCDW, which we refer to as the meltwater mixture. Shallow casts are removed from this analysis. To allow some variations of the water properties, we define a Gade envelope to determine whether a profile contains meltwater mixture.

Two criteria are defined to determine whether an individual profile “falls within the Gade envelope”: (1) In the layer with θ between 0.9°C and θ_{\max} , the slope in θ - S space must be equal to $3.5 \pm 0.1^\circ\text{C} (\text{psu})^{-1}$. This θ range is chosen so that the analysis focuses on water properties at the base of the thermocline, which are comparable to the draft of nearby ice shelves. The Gade line is approximately linear in this temperature range. Additionally, the slope is independent of the MCDW properties, or the choice of θ_{ocean} and S_{ocean} in equation (1). (2) At the depth where $S = 34.65 \text{ psu}$, we require $1.05 < \theta < 1.15^\circ\text{C}$. This allows for some θ - S variation of the mCDW. Both conditions (1) and (2) need to be satisfied. Broadening the Gade envelope allows more dives to meet the meltwater criteria; however, our sensitivity analysis to the size of the envelope did not show a qualitative difference in the geographic distribution of the meltwater mixture.

Figure 4 shows the locations of all dives that contain a portion of the water column falling within the Gade envelope. These dives are found predominantly west of the Wilkins Ice Shelf, in the Latady Trough, along the

western boundary of the Belgica Trough, along the continental shelf break west of the Belgica Trough, and in Eltanin Bay. The thickness of this meltwater mixture layer, indicated by symbol size in Figure 4, is typically between 100 and 200 m. The mean depth of that layer, indicated by colors in Figure 4, varies between 250 and 550 m. The deepest meltwater layer is found near the coast, adjacent to the Wilkins Ice Shelf and in the Eltanin Bay (Figure 4). The meltwater mixture, which occupies a range of densities between 27.9 and 28.1 kg m⁻³ (Figure S2), gradually shoals as it extends toward the shelf break along the western side of the troughs. This mixture is then found at progressively deeper depths moving to the west along the continental slope west of the Belgica Trough.

4. Discussion

The high density of seal data allows detailed observations of the circulation and water mass structure over the entire continental shelf of the Bellingshausen Sea; we focus on characteristics in the Belgica Trough, the main shelf break canyon in the western Bellingshausen Sea [Graham *et al.*, 2011].

Multiple synoptic sections across the shelf break indicate the presence of a shelf break current. The resolution of the seal data is relatively coarse compared to the typical scale of the ASC, which is often comparable to the Rossby radius of deformation, ~10 km. Nevertheless, the water mass distribution is indicative of a coherent ASC that is at least partially effective in separating offshore and onshore water. This is supported by Figures 2b, 2c, 2e, and 3a, which show that the offshore θ_{\max} is at depths shallower than the continental shelf. Yet water over the shelf is always modified from the offshore CDW properties. This modification is indicative of the Antarctic Slope Front (ASF) [Jacobs, 1991], which may indicate that the ASC is not limited to the “downstream” (western) side of the Belgica Trough. This is consistent with the hydrographic sections shown by Talbot [1988] and Jenkins and Jacobs [2008].

The seal data moves the easternmost observation of the ASC/ASF system from the Amundsen Sea [e.g., Wählin *et al.*, 2012] into the Bellingshausen Sea, suggesting that the origin lies closer to the West Antarctic Peninsula than previously suggested. Unlike in the Ross or Weddell Seas, where the ASC arises due to persistent along-slope easterly winds [Gill, 1973], in the Bellingshausen Sea a low-pressure system centered at 83°W generates predominantly southerly winds west of the Belgica Trough [Holland *et al.*, 2010]. Therefore, other mechanisms may give rise to this frontal structure, including frictional processes [Wählin *et al.*, 2012], the effects of tides [Flexas *et al.*, 2015], and eddy-induced transport of CDW onto the continental shelf [Thompson *et al.*, 2014].

Onshore of the shelf break, the appearance of the warmest waters along the eastern boundary of the Belgica Trough points to the importance of the trough in generating an onshore heat flux. Two-dimensional idealizations of the overturning circulation have been used to suggest the importance of an eddy transport of heat and mass over the continental slope and shelf in the Weddell Sea [Thompson *et al.*, 2014]. However, a closed, two-dimensional overturning circulation in the Bellingshausen Sea is likely an overly simplified picture in the absence of a deep outflow of AABW.

At 72°S, θ_{\max} differs as much as 0.2°C across the trough (Figure 3c). This difference is reduced to 0.05°C near the coast, where water warmer than 1.2°C is no longer detected (Figures 3e and 3f). This pattern is consistent with a cyclonic circulation, confined to narrow boundary currents. Warm and salty mCDW enters the Belgica Trough via the eastern boundary, where it entrains the cold and fresher water, then exits via the western boundary. Although modification could occur due to ice shelf meltwater, sea ice formation, or vertical mixing with Winter Water (WW) above the thermocline, our observations show that the most intense modification occurs below WW near the coast. Therefore, meltwater makes the greatest contribution to modification in the Belgica Trough. A careful examination of the vertical distribution of meltwater mixture shows that the θ_{\min} of the WW layer is always more than 100 m above the upper boundary of the meltwater layer; the mean separation is 206 m (Figure S3). Sea ice formation is another potential contributor to water mass modification; however, Talbot [1988] showed that winter formation of sea ice in the Bellingshausen Sea does not produce water dense enough to sink beneath the intruding CDW.

A striking feature of Figure 4 is that in addition to the near-coast profiles containing deep and thick meltwater layers, the highest density of meltwater away from the coast is confined to the western boundaries of the troughs. In particular, a pathway along the western side of the Belgica Trough, starting at 72°S, flows toward the shelf break and then extends west as far as 95°W. Moving along this pathway, the meltwater mixture becomes deeper, especially upon leaving the Belgica Trough. This may indicate an offshore export of the

meltwater due to bottom Ekman layer dynamics [Wählin *et al.*, 2012]. We acknowledge that the distribution of the observations varies from year to year (see Figure 1), although there are regions that contain data from more than 1 year. This inhomogeneous sampling could contribute to the observed meltwater distribution in Figure 4 if there is interannual variability in meltwater concentrations.

Identifying the exact source of meltwater is beyond the scope of this paper; however, the meltwater mixture distributions suggest possible sources of ice shelf meltwater in this region. Figure 3e sits in front of Venable Ice Shelf and is a source of meltwater as indicated in Figure 4. Preliminary estimation suggests the highest meltwater fraction occurs in front of Venable Ice Shelf as well (not shown). The section near the coast in Eltanin Bay (Figure 3f) also shows a large proportion of meltwater. This meltwater could originate from the Venable Ice Shelf since the easternmost extent of this ice shelf lies to the east of a ridge that defines the northwestern boundary of the deep Eltanin Bay. Additionally, a westward coastal current may carry meltwater from ice shelves east of Belgica Trough to Eltanin Bay [Moffat *et al.*, 2008].

The nonuniform sampling by the seals between different years makes it difficult to infer trends in meltwater discharge rates. However, near the coast temporal variability is observed with a deeper and thicker meltwater layer in 2013–2014, as compared to 2009 (Figure 4 inserts). Away from the coast, the meltwater layer becomes shallower within the Belgica Trough, most likely due to mixing with overlying waters. The deepest meltwater at the shelf break, west of 90°W, all came from a single year, 2010. During 2010 there were no near-coast profiles collected by the seals; therefore, we are unable to document whether this corresponds to interannual variability in meltwater discharge rates.

5. Conclusions

Nearly 20,000 hydrographic profiles from instrumented seals collected between 2007 and 2014 were analyzed to highlight spatial patterns in circulation pathways and meltwater contributions in the western Bellingshausen Sea. Warm modified Circumpolar Deep Water (mCDW) 3°C above the freezing point is found on the continental shelf and extends to the coast in a narrow eastern boundary current, accompanied by cooling and freshening of the temperature and salinity maxima, respectively. Western boundary currents in troughs entrain ice shelf meltwater near the coast and carry the mCDW-meltwater mixture to the shelf break. This comprehensive data set highlights the importance of boundary currents in (i) modifying CDW across an established shelf break frontal system, (ii) delivering warm water toward the major ice shelves, and (iii) exporting meltwater mixtures toward the open ocean and potentially westward toward the Amundsen Sea within the Antarctic Slope Current. The distribution of meltwater mixtures supports the high basal melt rate and thinning of Venable Ice Shelf detected by satellite observations, but more importantly, emphasizes the need to monitor fine-scale ocean circulation features to understand future changes in the West Antarctic Ice Sheet.

Acknowledgments

The MEOP consortium coordinates several seal-tagging national programs to provide a comprehensive oceanographic coverage in Polar Regions (<http://www.meop.net/>). Bellingshausen Sea data were produced with support from the Alfred Wegener Institute Helmholtz Centre for Polar and Marine Research (GER), the Instituto Antártico Argentino (ARG), the National Oceanographic Partnership Program (USA), and the Brazilian National Research Council (BRA). Data and information can be accessed at www.coriolis.eu.org with details in the supporting information. We would like to thank the anonymous reviewers for their constructive comments. A.F.T. acknowledges support by NSF award OPP-1246460. M.M.F. is supported by the NASA Postdoctoral Program administered by Oak Ridge Associated Universities. This research was in part carried out at the Jet Propulsion Laboratory, California Institute of Technology, under a contract with NASA.

References

- Aoki, S., S. R. Rintoul, S. Ushio, S. Watanabe, and N. L. Bindoff (2005), Freshening of the Adélie land bottom water near 140°E, *Geophys. Res. Lett.*, *32*, L23601, doi:10.1029/2005GL024246.
- Arndt, J. E., et al. (2013), The International Bathymetric Chart of the Southern Ocean (IBCSO) version 1.0—A new bathymetric compilation covering circum-Antarctic waters, *Geophys. Res. Lett.*, *40*, 3111–3117, doi:10.1002/grl.50413.
- Arneborg, L., A. Wählin, G. Björk, B. Liljebladh, and A. Orsi (2012), Persistent inflow of warm water onto the central Amundsen shelf, *Nat. Geosci.*, *5*, 876–880, doi:10.1038/ngeo1644.
- Boehme, L., P. Lovell, M. Biuw, F. Roquet, J. Nicholson, S. E. Thorpe, M. P. Meredith, and M. Fedak (2009), Technical note: Animal-borne CTD-satellite relay data loggers for real-time oceanographic data collection, *Ocean Sci.*, *5*(4), 685–695, doi:10.5194/osd-6-1261-2009.
- Costa, D. P., J. M. Klinck, E. E. Hofmann, M. S. Dinniman, and J. M. Burns (2008), Upper ocean variability in west Antarctic Peninsula continental shelf waters as measured using instrumented seals, *Deep Sea Res., Part II*, *55*, 323–337, doi:10.1016/j.dsr2.2007.11.003.
- Dutrieux, P., J. De Rydt, A. Jenkins, P. R. Holland, H. K. Ha, S. H. Lee, E. J. Steig, Q. Ding, E. P. Abrahamson, and M. Schröder (2014), Strong sensitivity of Pine Island Ice-Shelf melting to climatic variability, *Science*, *343*, 174–178, doi:10.1126/science.1244341.
- Flexas, M. M., M. P. Schodlok, L. Padman, D. Menemenlis, and A. H. Orsi (2015), Role of tides on the formation of the Antarctic slope front at the Weddell-Scotia confluence, *J. Geophys. Res. Oceans*, *120*, 3658–3680, doi:10.1002/2014JC010372.
- Gade, H. G. (1979), Melting of ice in sea water: A primitive model with application to the Antarctic ice shelf and icebergs, *J. Phys. Oceanogr.*, *9*, 189–198, doi:10.1175/1520-0485(1979)009<0189:MOISW>2.0.CO;2.
- Gill, A. (1973), Circulation and bottom water production in the Weddell Sea, *Deep Sea Res.*, *20*(2), 111–140, doi:10.1016/0011-7471(73)90048-X.
- Gille, S. T. (2008), Decadal-scale temperature trends in the Southern Hemisphere ocean, *J. Clim.*, *21*, 4749–4765, doi:10.1175/2008JCLI2131.1.
- Graham, A. G., F. Nitsche, and R. D. Larter (2011), An improved bathymetry compilation for the Bellingshausen Sea, Antarctica, to inform ice-sheet and ocean models, *Cryosphere*, *5*, 95–106, doi:10.5194/tc-5-95-2011.
- Holland, P. R., A. Jenkins, and D. M. Holland (2010), Ice and ocean processes in the Bellingshausen Sea, Antarctica, *J. Geophys. Res.*, *115*, C05020, doi:10.1029/2008JC005219.

- Jacobs, S. S. (1991), On the nature and significance of the Antarctic Slope Front, *Mar. Chem.*, *35*, 9–24, doi:10.1016/S0304-4203(09)90005-6.
- Jacobs, S. S., H. H. Hellmer, and A. Jenkins (1996), Antarctic ice sheet melting in the Southeast Pacific, *Geophys. Res. Lett.*, *23*, 957–960, doi:10.1029/96GL00723.
- Jenkins, A. (1999), The impact of melting ice on ocean waters, *J. Phys. Oceanogr.*, *29*, 2370–2381, doi:10.1175/1520-0485(1999)029<2370:TIOPIO>2.0.CO;2.
- Jenkins, A., and S. Jacobs (2008), Circulation and melting beneath George VI Ice Shelf, Antarctica, *J. Geophys. Res.*, *113*, C04013, doi:10.1029/2007JC004449.
- McIntyre, T., H. Bornemann, P. N. de Bruyn, R. R. Reisinger, D. Steinhage, M. E. Márquez, M. N. Bester, and J. Plötz (2014), Environmental influences on the at-sea behaviour of a major consumer, *Mirounga leonina*, in a rapidly changing environment, *Pol. Res.*, *33*, 23808, doi:10.3402/polar.v33.23808.
- Moffat, C., R. C. Beardsley, B. Owens, and N. Van Lipzig (2008), A first description of the Antarctic Peninsula Coastal Current, *Deep Sea Res., Part II*, *55*, 277–293, doi:10.1016/j.dsr2.2007.10.003.
- Nakayama, Y., M. Schröder, and H. H. Hellmer (2013), From circumpolar deep water to the glacial meltwater plume on the eastern Amundsen shelf, *Deep Sea Res., Part I*, *77*, 50–62, doi:10.1016/j.dsr.2013.04.001.
- Nakayama, Y., R. Timmermann, C. B. Rodehacke, M. Schröder, and H. H. Hellmer (2014), Modeling the spreading of glacial meltwater from the Amundsen and Bellingshausen Seas, *Geophys. Res. Lett.*, *41*, 7942–7949, doi:10.1002/2014GL061600.
- Orsi, A. H., T. Whitworth III, and W. D. Nowlin Jr. (1995), On the meridional extent and fronts of the Antarctic circumpolar current, *Deep Sea Res., Part I*, *42*, 641–673, doi:10.1016/0967-0637(95)00021-W.
- Padman, L., et al. (2012), Oceanic controls on the mass balance of Wilkins Ice Shelf, Antarctica, *J. Geophys. Res.*, *117*, C01010, doi:10.1029/2011JC007301.
- Paolo, F. S., H. A. Fricker, and L. Padman (2015), Volume loss from Antarctic ice shelves is accelerating, *Science*, *348*, 327–331, doi:10.1126/science.aaa0940.
- Pritchard, H., S. Ligtenberg, H. Fricker, D. Vaughan, M. Van den Broeke, and L. Padman (2012), Antarctic ice-sheet loss driven by basal melting of ice shelves, *Nature*, *484*, 502–505, doi:10.1038/nature10968.
- Purkey, S. G., and G. C. Johnson (2013), Antarctic Bottom Water warming and freshening: Contributions to sea level rise, ocean freshwater budgets, and global heat gain, *J. Clim.*, *26*, 6105–6122, doi:10.1175/JCLI-D-12-00834.1.
- Rignot, E., S. Jacobs, J. Mouginot, and B. Scheuchl (2013), Ice-shelf melting around Antarctica, *Science*, *341*, 266–270, doi:10.1126/science.1235798.
- Rintoul, S. R. (2007), Rapid freshening of Antarctic Bottom Water formed in the Indian and Pacific Oceans, *Geophys. Res. Lett.*, *34*, L06606, doi:10.1029/2006GL028550.
- Roquet, F., J.-B. Charrassin, S. Marchand, L. Boehme, M. Fedak, G. Reverdin, and C. Guinet (2011), Delayed-mode calibration of hydrographic data obtained from animal-borne Satellite Relay Data Loggers, *J. Atmos. Oceanic Technol.*, *28*, 787–801, doi:10.1175/2010JTECHO801.1.
- Roquet, F., et al. (2013), Estimates of the Southern Ocean general circulation improved by animal-borne instruments, *Geophys. Res. Lett.*, *40*, 6176–6180, doi:10.1002/2013GL058304.
- Schmidtko, S., K. J. Heywood, A. F. Thompson, and S. Aoki (2014), Multidecadal warming of Antarctic waters, *Science*, *346*, 1227–1231, doi:10.1126/science.1256117.
- Talbot, M. H. (1988), Oceanic environment of George VI Ice Shelf, Antarctic peninsula, *Ann. Glaciol.*, *11*, 161–164.
- Thompson, A. F., K. J. Heywood, S. Schmidtko, and A. L. Stewart (2014), Eddy transport as a key component of the Antarctic overturning circulation, *Nat. Geosci.*, *7*, 879–884, doi:10.1038/ngeo2289.
- Wåhlin, A., X. Yuan, G. Björk, and C. Nohr (2010), Inflow of warm Circumpolar Deep Water in the central Amundsen shelf, *J. Phys. Oceanogr.*, *40*, 1427–1434, doi:10.1175/2010JPO4431.1.
- Wåhlin, A., R. Muench, L. Arneborg, G. Björk, H. Ha, S. Lee, and H. Alsén (2012), Some implications of Ekman layer dynamics for cross-shelf exchange in the Amundsen Sea, *J. Phys. Oceanogr.*, *42*(9), 1461–1474, doi:10.1175/JPO-D-11-041.1.
- Wåhlin, A., O. Kalén, L. Arneborg, G. Björk, G. Carvajal, H. Ha, T. Kim, S. Lee, J. Lee, and C. Stranne (2013), Variability of warm deep water inflow in a submarine trough on the Amundsen Sea shelf, *J. Phys. Oceanogr.*, *43*, 2054–2070, doi:10.1175/JPO-D-12-0157.1.
- Walker, D. P., A. Jenkins, K. M. Assmann, D. R. Shoosmith, and M. A. Brandon (2013), Oceanographic observations at the shelf break of the Amundsen Sea, Antarctica, *J. Geophys. Res. Oceans*, *118*, 2906–2918, doi:10.1002/jgrc.20212.
- Whitworth, T., A. H. Orsi, S.-J. Kim, W. D. Nowlin, and R. A. Locarnini (1998), Water masses and mixing near the Antarctic slope front, in *Ocean, Ice, and Atmosphere: Interactions at the Antarctic Continental Margin*, edited by S. S. Jacobs and R. F. Weiss, pp. 1–27, AGU, Washington, D. C., doi:10.1029/AR075p0001.
- Wouters, B., A. Martín-Español, V. Helm, T. Flament, J. van Wessem, S. Ligtenberg, M. van den Broeke, and J. Bamber (2015), Dynamic thinning of glaciers on the southern Antarctic Peninsula, *Science*, *348*(6237), 899–903, doi:10.1126/science.aaa5727.